Statistical Modeling of Corrosion-Induced Wirebond Failure

N. Robert Sorensen
Jeffrey W. Braithwaite
Sandia National Laboratories
Albuquerque, NM 87185-0340

INTRODUCTION

When unforeseen materials-degradation problems are encountered in many electronic devices used in defense applications, the typical approach is to evaluate the severity, estimate any consequence, and then, if needed, replace the material, change the environment, or retrofit entire components. As such, the need for accurately predicting long-term reliability has not strictly existed. However, as these devices continue to age, interest grows in extending their service life past the nominal design life. In addition, sometimes functional hardware is changed out because of uncertainty in the consequence assessment. As such, an effective capability to predict long-term reliability over extended time periods is now desirable.

A key aspect to characterizing the reliability of electronic components involves the aging of materials. One of the significant chemical degradation mechanisms that affects many components is atmospheric corrosion. A list of the types of devices that have been observed to be susceptible to this form of corrosion are presented in Table 1. Figure 2 includes several related photographs of actual field occurrences.

This paper describes the initial results of a project that is the near-term portion of a much larger and integrated program to develop effective analytical tools for predicting the effect of atmospheric corrosion on the reliability of electronic devices. In general terms, this activity involves the development of "back end" tools of the program: the statistical treatment of stochastic corrosion data and the subsequent analysis of reliability. As part of this project, an early assessment is being made relative to the applicability of a standard reliability methodology to corrosion-based degradation. This project complements two other ongoing corrosion tasks at Sandia: the long-term development of fundamental corrosion models and the mid-term development of phenomenological models. That is, the methodology developed in all three activities must be incorporated into a comprehensive modeling capability to permit practical problems to be addressed.

---

*This work was supported by the United States Department of Energy under Contract DE-AC04-94AL85000. Sandia is a multiprogram laboratory operated by Sandia Corporation, a Lockheed Martin Company, for the United States Department of Energy

DISCLAIMER

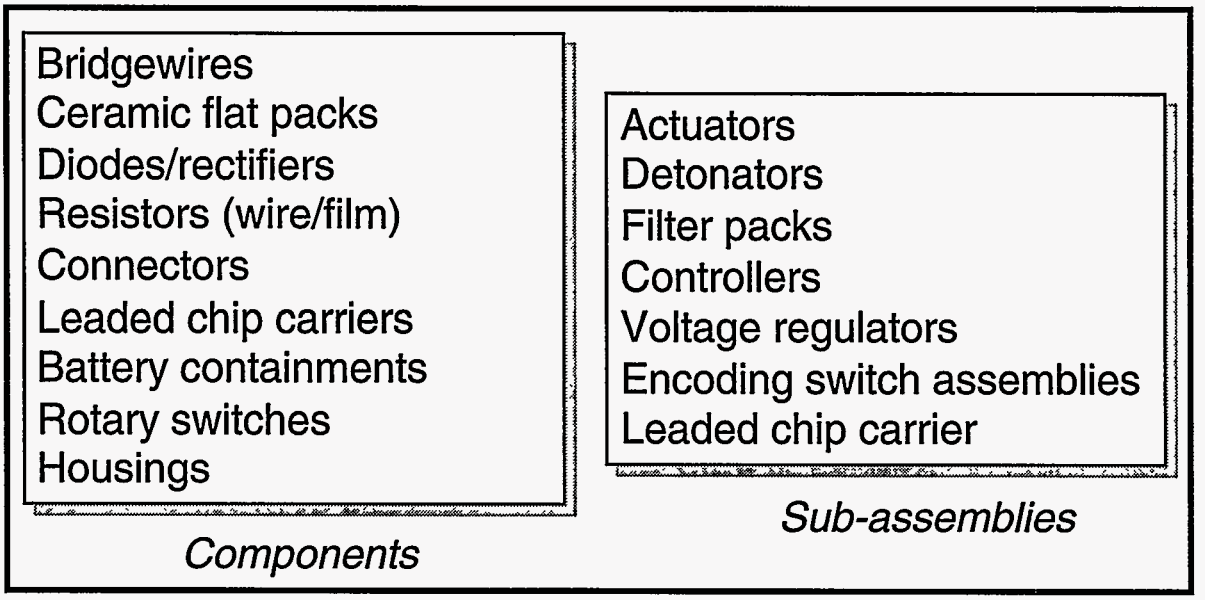

Figure 1. *List of many of the military electronic devices that have been affected by atmospheric corrosion during production or storage.*

The specific objectives of this work were to experimentally characterize the atmospheric corrosion of aluminum-gold wirebonds and to develop a statistical-based model that describes the effect of the resulting stochastic process on the reliability of a selected electronic assembly. This particular corrosion process was attractive for this initial study because of the following reasons: (1) actual field failures have occurred, (2) an incompatible materials combination exists, (3) the environment can be simulated in the laboratory, (4) a statistically significant number of joints can be studied, (5) failure detection is relatively easy, and (6) the process is clearly stochastic. In general, corrosion of the wirebond produces an increase in electrical resistance across the interface until an actual open occurs. In the limit, component failure will occur due to a voltage drop that will either prevent proper operation of an internal electrical circuit or not supply adequately high voltage levels for external needs.

The basis for making valid predictions consists of a detailed understanding of the relevant phenomenology and a database from which to develop and validate descriptive mathematical models. How the various aspects of this foundation are formed is presented in Figure 3. The experimental characterization of Al/Au atmospheric corrosion that was performed included a mandatory attempt at accelerated aging. Because of the near-term emphasis of this project, the modeling focused on empirical and statistical treatments of the corrosion data. The modeling steps that were followed are depicted in Figure 4 which shows the three required principal activities consist of (a) the development and validation of empirical models that describe the effects of environmental parameters on corrosion rate, and (b) the formulation and validation of a reliability-prediction model using the accelerated aging data and long-term field information as it becomes available. Results obtained to date on all these activities are presented in the remainder of this paper.

a. galvanic corrosion of igniter bridgewire

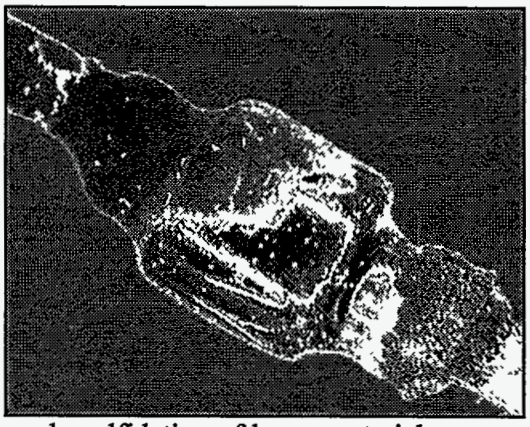

b. sulfidation of braze material spread across a diode

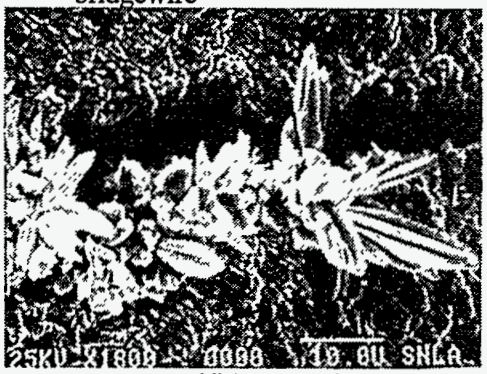

c. copper sulfide crystals growing from crack in a leaded-chip carrier

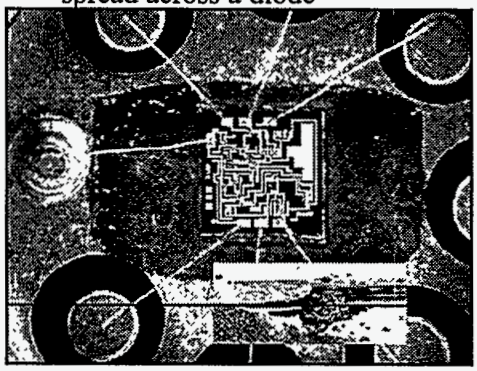

d. open Al/Au wirebonds in an op amp that were exposed to moisture and contamination

Figure 2. Photographs of several electronic devices that have failed due to atmospheric corrosion.

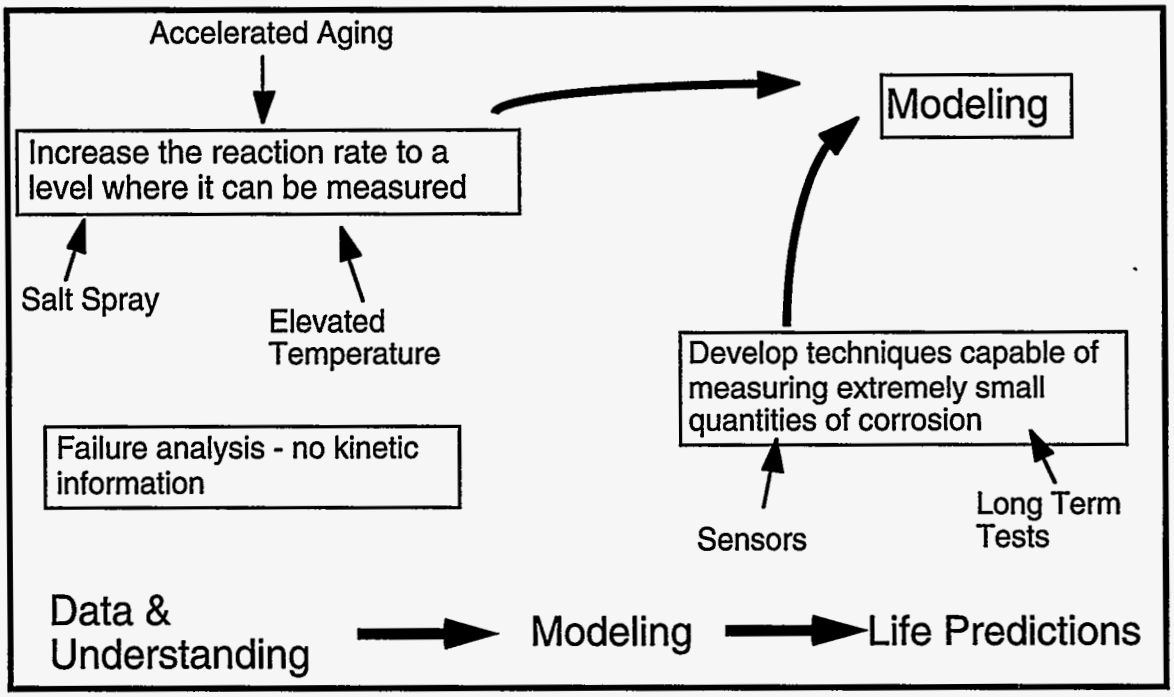

Figure 3. *Flowchart showing the basis for making valid predictions.*

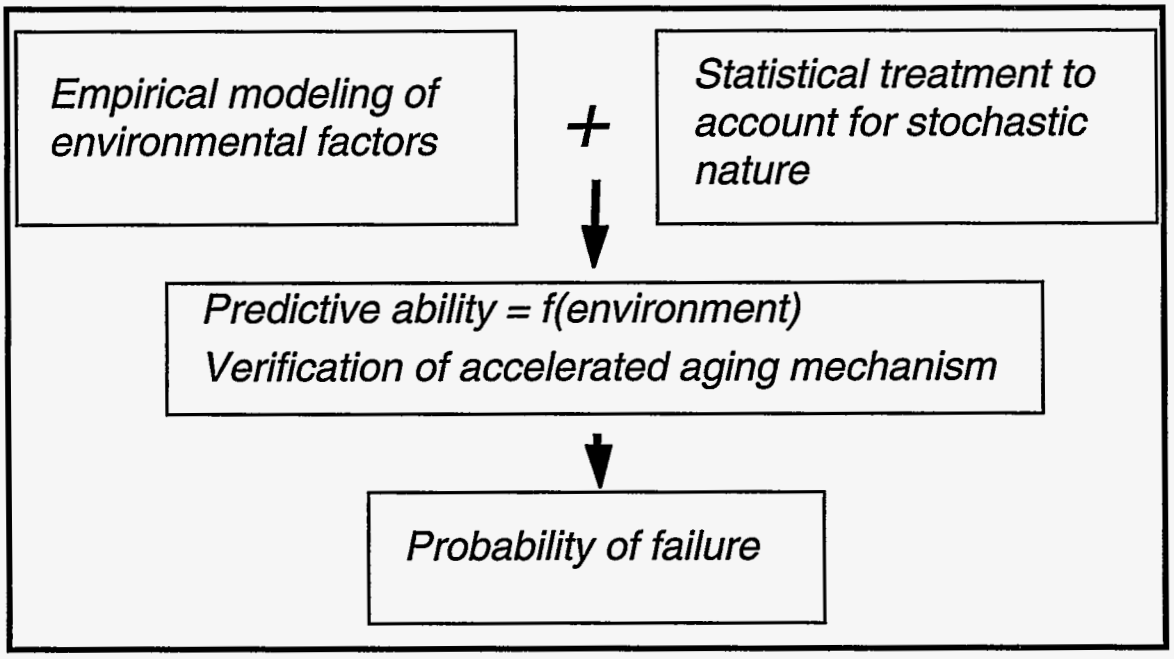

Figure 4. *Graphical representation of the modeling portion of this study.*

EXPERIMENTAL PROCEDURES

Wirebond Test Vehicle

The stochastic nature of aluminum wirebond corrosion required that a large number of wirebonds be tested. To satisfy this need, the test device used to monitor corrosion was a ceramic chip carrier containing either 40 or 64 gold pads. Al wires (1 mil diameter) were attached in a daisy chain configuration around the chip. A photograph of the device is shown in Figure 5. Wires were soldered to the leads of the test chip and were used to monitor the resistance of each bond wire. By measuring the resistance between every set of adjacent pads, the status of each wire bond was independently followed. One wirebond was physically removed between the first and last bond pads to prevent the measurement of an artificial resistance (backward through the entire chain). A schematic diagram of the automated data collection system is given in Figure 6. The leads from the test chip were connected into a 100 channel Keithley scanner. Resistance was measured with a Keithley digital voltmeter using a 4-lead measurement setup. The computer was interfaced with both the scanner and the digital voltmeter to scan all of the wirebonds and collect resistance data. As corrosion degraded the Al wire, the resistance increased until open circuit occurred. For consistency, failure was defined as a resistance greater than 100 Ω. This assumption was reasonable in that the resistance of individual wirebonds increased only marginally prior to complete open. This result also means that resistance increase cannot be used as an effective measure of incremental attack.

Environmental Exposure

The prime objective of this activity was to accelerate aging under controlled environmental conditions such that the effects of chloride contamination, humidity and temperature can be characterized in reasonable periods of time. The procedures used to control these parameters are described below. However, at this time, only the chloride concentration has been extensively studied.

Chloride Contamination

In order to accelerate corrosion of the Al wirebonds, the surface of the test vehicle was coated with varying amounts of NaCl. NaCl was dissolved in ethanol to make a saturated solution and was applied to each chip with an airbrush. Initially, water was used as the solvent for the NaCl, but, due to the slow evaporation rate of the water, an excessive amount of corrosion occurred during the spraying operation. This caused failure of most of the wirebonds prior to elevated humidity exposure. By dissolving NaCl in alcohol, evaporation was much more rapid, leaving the wirebonds intact. A quartz crystal microbalance (QCM) employing a gold coated AT-cut quartz crystal was mounted next to the test chip to monitor the deposition rate and final NaCl film thickness. The level of contamination was controlled by varying the number of repetitive applications of the NaCl/EtOH solution.

Humidity Exposure.

After the samples were contaminated with NaCl, each was allowed to completely dry. To prevent condensation caused by the introduction of a cold device into a warm, high humidity environment, each chip was preheated in an oven at 50 °C. Aging was performed in a Blue M model VP-100RAT humidity chamber. The chamber was held at constant humidity throughout any particular test. A shield was placed above the sample to prevent water drops from falling on the sample surface.

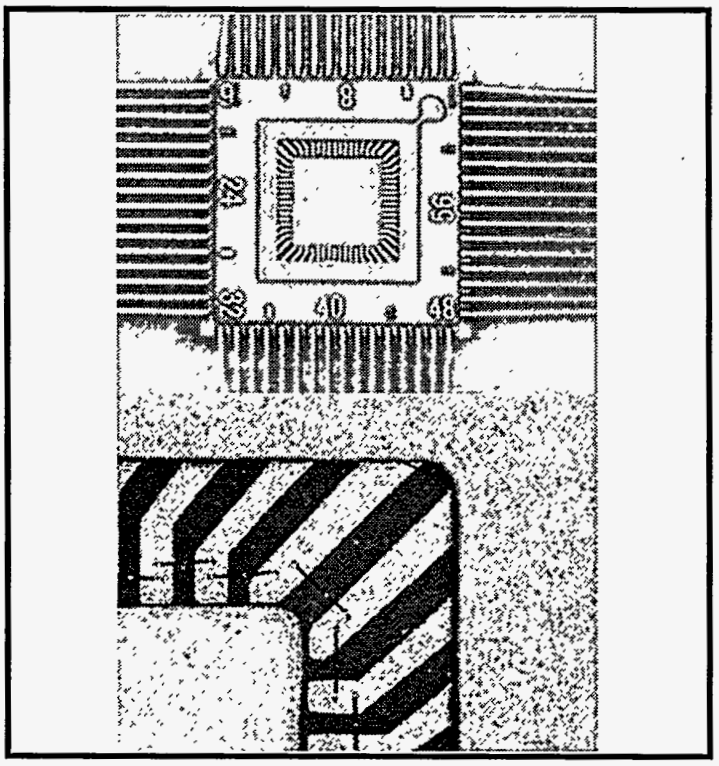

Figure 5. Photograph of test chip used to monitor corrosion induced failure of Al wirebonds.

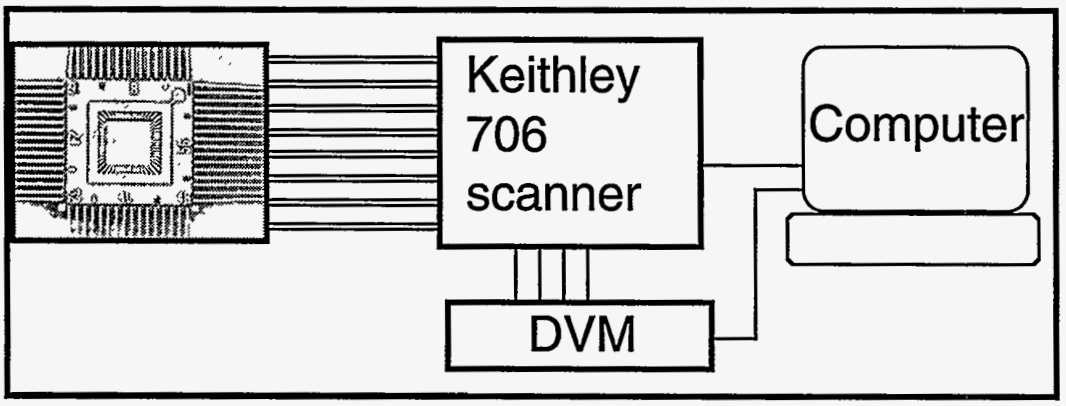

***Figure 6.** Schematic of the automated data collection system.*

CHARACTERIZATION OF WIREBOND FAILURE

The stochastic nature of atmospheric Al wirebond corrosion is shown in Figure 7. All of the wirebonds on the chip were subjected to the same environment. Note that some of the wires were severely corroded, while another, directly adjacent wire was essentially unattacked.

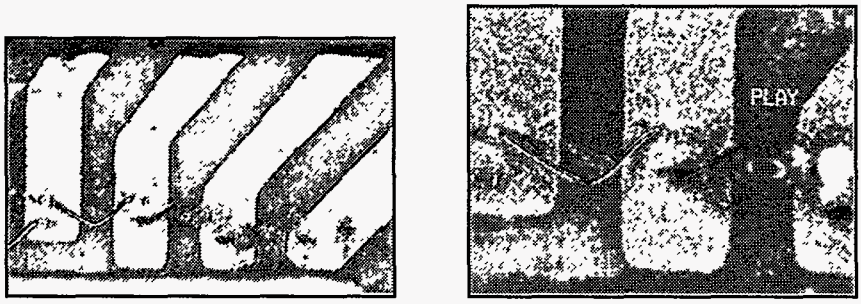

***Figure** 7. Aluminum wirebonds on corrosion test vehicle following exposure to relative humidity environment. Note that severely corroded wirebonds may be found next to essentially pristine wires.*

The concentration of Cl on the surface of the Al/Au wirebond was critical to the corrosion or failure rate. Figure 8 shows the change in mass, measured with a quartz crystal microbalance, for 6 successive applications of NaCl. The slope in Figure 8b is constant between the second and sixth application, giving a deposition rate of ~ 1.8 $\mu g/cm^2$/application. During the first application, a larger quantity of NaCl was deposited (5 $\mu g/ cm^2$), which may have been the result of the application occurring on a gold surface rather than a NaCl covered gold surface. By using the QCM to follow the deposition process, an accurate measure of surface NaCl was obtained.

Both resistance *vs.* time and time-to-failure data were collected for each channel or wirebond. The resistance data were used only as reference to verify failure because, as noted earlier, degradation could not be monitored by resistance increase. Cumulative failure plots for three levels of Cl contamination are presented in Figure 9. Note the difference in failure rate between the sample receiving 6 coats of NaCl and that receiving 4 coats. For the former sample, 80% of the wirebonds failed within 10 hours, while the latter exhibited fewer than 20% failures after aging for more than 80 hours. The failures for 6 coats and 5 seconds continuous both occur at relatively short times, with little or no apparent induction time. The lack of an induction time is inconsistent with the physical process (localized corrosion of Al) as observed in field electronics and thus indicates that the rate is being overly accelerated in this experiment. That is, from field data, an induction time does exist for corrosion of Al wirebonds, leading to a concern that the corrosion mechanism has been changed for our accelerated tests. This subject is addressed further in the modeling section.

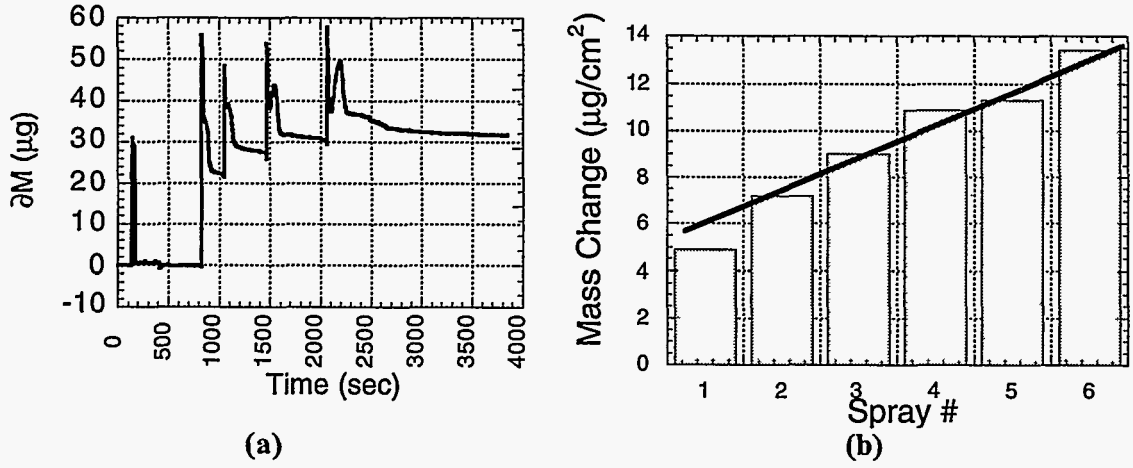

Figure 8. Data showing NaCl deposition process. Data in (a) represent actual QCM data, and (b) presents mass change as a function of number of applications. The NaCl is applied as an ethanol solution and the ethanol is allowed to evaporate. The mass change following the evaporation process is attributed to deposition of NaCl.

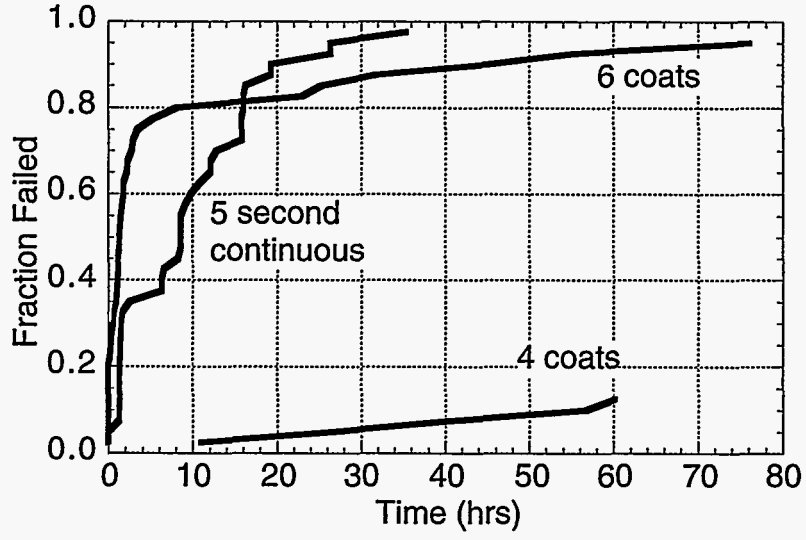

Figure 9. Cumulative failure as a function of time for three chloride levels.

Based on the rate data obtained, including that shown in Figure 9, an empirical sigmoidal relationship was generated that describes the effect of chloride contamination level on the relative time-to-failure (TTF) that is shown in Figure 10. The TTF term is defined as the fraction of wirebonds failed at a given time normalized by the maximum rate observed (that obtained when the [Cl] > 20 μg/ cm^2). At low concentrations, there is insufficient Cl present to induce breakdown of the passive layer, and the resulting failure rate is very low. In this system, the corresponding minimum or critical Cl concentration is about 10 μg/cm^2 for initiating corrosion in real time. As the Cl level increases and reaches levels necessary to promote pitting initiation, the failure rate increases. At some point, the Cl effect saturates such that further increases have little effect on the kinetics.

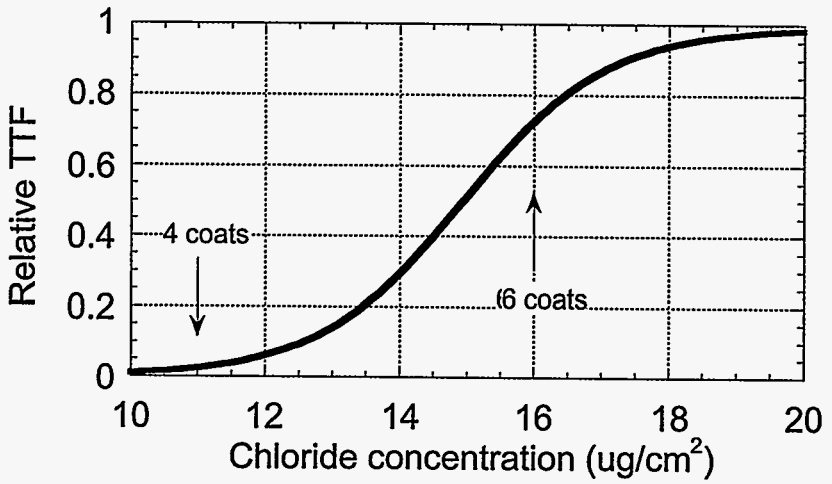

Figure 10. Empirical relationship of the effect of chloride contamination level on the relative time-to-failure of Al/Au wirebonds.

Similarly, the effect of relative humidity on the corrosion rate can be defined by the sigmoidal relationship in Figure 11. At low levels of humidity, the reaction is basically a gas-metal reaction and the rate is low. With increased humidity, there is an increase in the number of adsorbed layers of water on the surface. At some point, the adsorbed layer takes on characteristics of a bulk electrolyte, the corrosion process becomes electrochemical and the corrosion rate rises sharply. Based on literature results for atmospheric corrosion processes, the transition normally occurs at about 60% RH, above which the corrosion proceeds much faster. Once a critical number of monolayers of water exist on the surface, further increase in relative humidity has minimal effect on the failure rate.

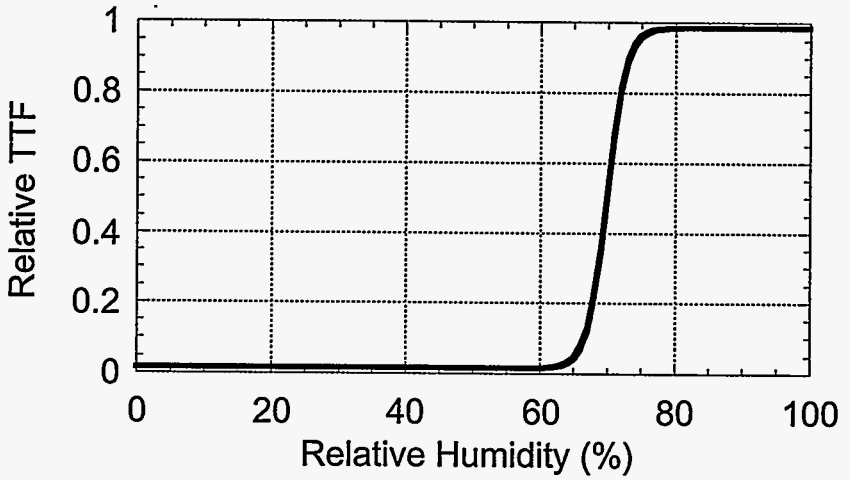

Figure 11. *Empirical relationship of the effect of humidity on the relative time-to-failure of Al/Au wirebonds.*

Based on these results and general literature information, an empirical equation was defined to describe the time to failure (t_f) as a function of relative humidity (RH), surface chloride concentration (Cl^-), and temperature:

$$t_f = k \bullet f(RH) \bullet g([Cl^-]) \bullet \exp(-E_a/RT)$$

where f and g represent independent sigmoidal functions presented above and the temperature dependence follows an Arrhenius relationship (consistent with an activated process). In this way, effects of humidity, chloride concentration and temperature can be separately addressed. In the calculations that follow an activation energy of 5 kcal/mole that is reasonable for atmospheric corrosion was used. The assumption that temperature can be simply treated with an Arrhenius relationship is probably adequate at this point in the model development because of how humidity is being treated. That is, atmospheric corrosion can sometimes show apparent negative activation energy values because higher temperatures can reduce the moisture on the surface. However, the use of relative humidity precludes this complication.

STATISTICAL ANALYSIS OF COMPONENT RELIABILITY

The objective of this part of the project was to demonstrate how stochastic corrosion information can be used in component reliability calculations. In this exercise, the wirebond failure information described in the previous section that was obtained under greatly accelerated conditions was used. The specific steps that were followed consisted of the following:

1. define a conceptual integrated circuit component assembly that contains Al/Au wirebonds
2. select two different environments to simulate
3. calculate applicable environmental deceleration factors relative to the accelerated aging environment
4. determine failure distributions for each environment
5. perform a "Monte Carlo" statistical analysis to determine the component failure distribution

To facilitate this activity, a hypothetical electronic assembly (Figure 12) was selected and a number of simplifying assumptions made. The functional part of this assembly that is of interest is composed of 25 integrated circuits (IC) with each integrated circuit containing 8 wirebonds. The key assumptions relative to failure include:

- the hermeticity of all 25 IC's is compromised permitting exposure to an external environment
- all 200 wirebonds (25 IC's x 8 wirebonds/IC) have same susceptibility to corrosion
- assembly failure occurs when either of the 2 power leads on 5 critical integrated circuits open (this assumption means that only 10 specific wirebonds have a direct or first order effect on the functionality of the assembly)

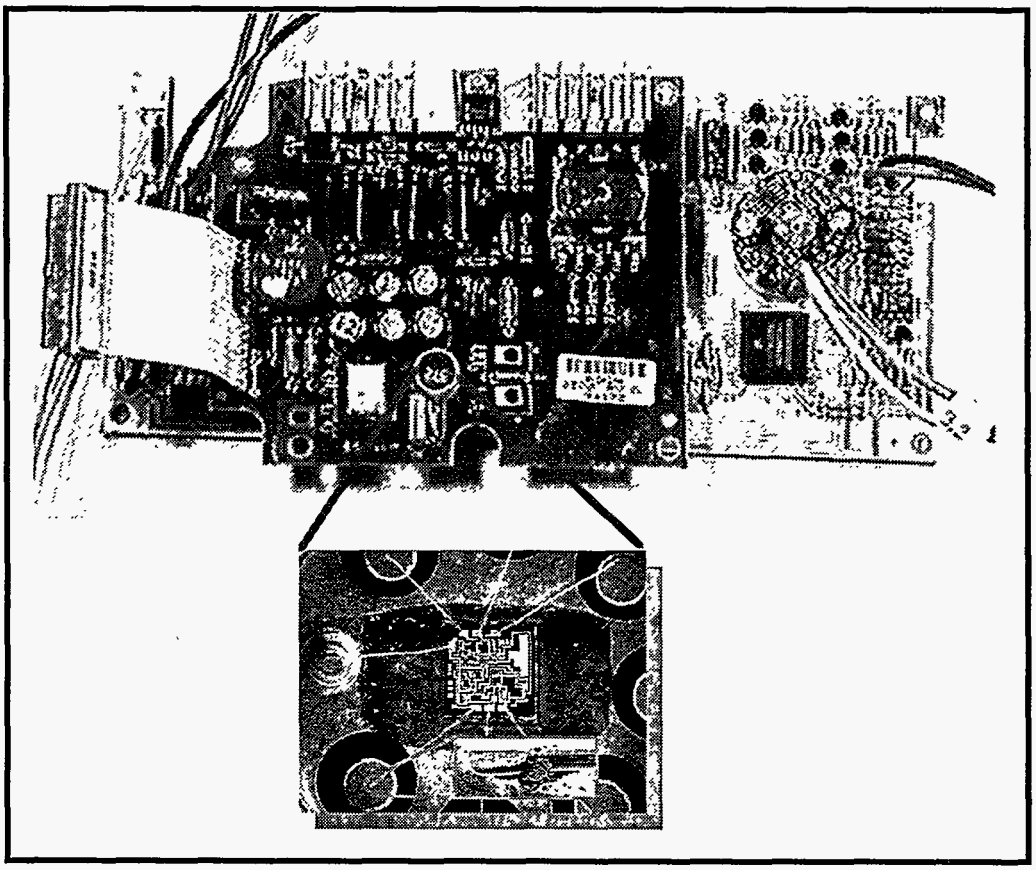

Figure 12. *Photograph of the hypothetical electronic assembly that contains 20 integrated circuits, each with 8 susceptible Al/Au wirebonds (breakout).*

This greatly simplified approach was necessary because the models needed to describe the complex time-based degradation of the actual constituents (e.g., resistors, diodes, op amps, connectors) and their associated interactions with the system are simply not yet available. In addition, the objective of this exercise is to demonstrate the analytical methodology and not address a specific issue.

The second and third steps listed above consisted of selecting two contrasting environments and calculating relevant wirebond failure distributions. A desert and seacoast environment were chosen for the simulation. The goal was then to show how an environmental difference could affect reliability. The assumed conditions for the three environments (accelerated aging, desert, and seacoast) are listed in Table 1. Because of the critical role of chloride contamination level and the existence of a minimum level needed to induce wirebond failure, the value associated with the desert environment was chosen to represent that possible if contamination occurred during manufacturing, whereas the seacoast level could exist if similar contamination was present plus some equilibration with the saline atmosphere. Both of the relative chloride levels given in the table represent the concentration above the critical concentration for passive film breakdown of 10 $\mu g/cm^2$.

Table 1. Environmental conditions used in the reliability calculations

Parameter	*Accelerated Conditions*	*Desert*	*Seacoast*
Temperature (°C)	40	28	15
Relative Humidity (%)	85	30	80
Relative Chloride Level (μg/cm^2)	6	0.1	0.5

Using the data and the empirical equation presented in the previous section, the deceleration factors for each of the environments to be simulated relative to the accelerated test conditions were calculated. The position of the values listed in Table 1 for both simulated environments on the relative failure rate response for the humidity and chloride parameters is shown graphically in Figures 13 and 14. The quantitative results are presented in Table 2. Figure 14 is an expanded view of Figure 10 with the chloride level again being relative to the critical concentration for corrosion initiation. Clearly, aging extrapolations of the magnitude given in Table 2 are not justified by the very limited database established to date. That is, less aggressive accelerating conditions coupled with substantially more understanding are required before we can have confidence that the mechanisms operating under the accelerated conditions are applicable to the actual environment. As such, quantitative conclusions based on these results should not be considered as valid.

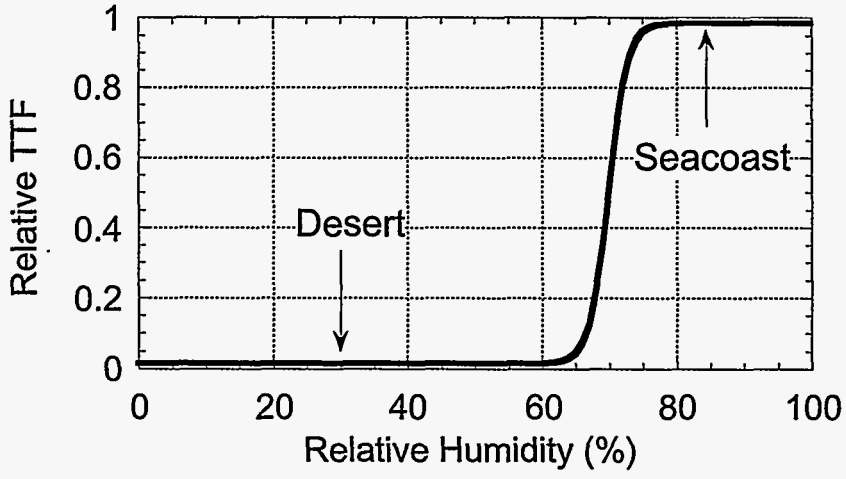

Figure 13. *Position of the selected relative humidity parameters on the wirebond relative failure rate.*

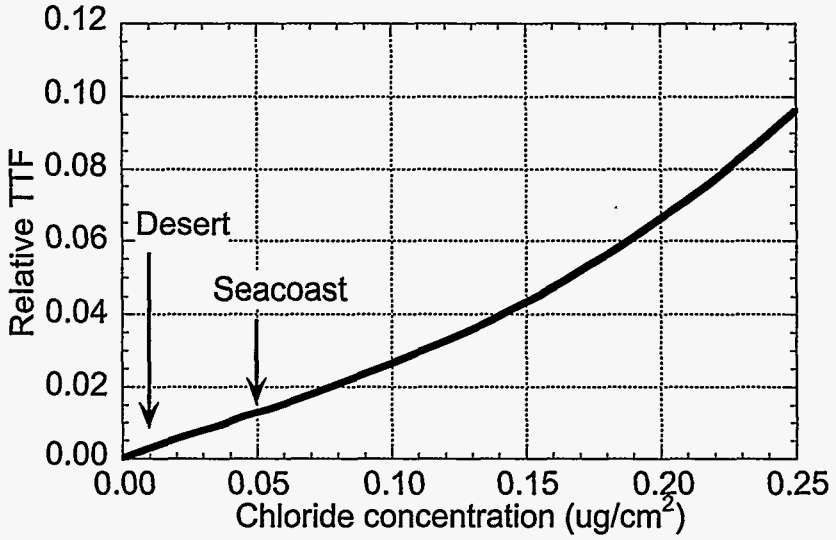

Figure 14. *Position of the selected chloride contamination parameters on the wirebond relative failure rate.*

Table 2. *Individual and total deceleration factors associated with the two simulated environments*

Parameter	*Desert*	*Seacoast*
Temperature	1.3	2
Relative Humidity	80	1
Chloride Contamination	275	55
Total	30,000	110

The experimental failure data obtained under accelerated conditions were then rescaled for each environment using the Table 2 deceleration factors and empirically fit to several standard distributions. As shown in Figures 15 and 16, the Weibull distribution adequately describe these extrapolated failure data. The calculated Weibull parameters are also included in the figures: alpha (characteristic life) and beta (shape factor or modulus). The characteristic life is a measure of average life and the shape factor is a measure of the change in failure rate with time. An expanded view of the data in Figure 15 is given in Figure 17. The linearity of the majority of the failure data (a constant failure rate) visually validates the calculated Weibull shape factor of 1 along with the lack of any induction period. The linear rate and lack of induction is not consistent with field experience and is probably an artifact of the overly aggressive accelerated conditions used. Typically, modulus values of 3 or greater (increasing failure rate) are observed for these types of failures. Of note, a modulus of 3 was produced for this test configuration except under inundated condition with dilute NaCl aqueous solutions.

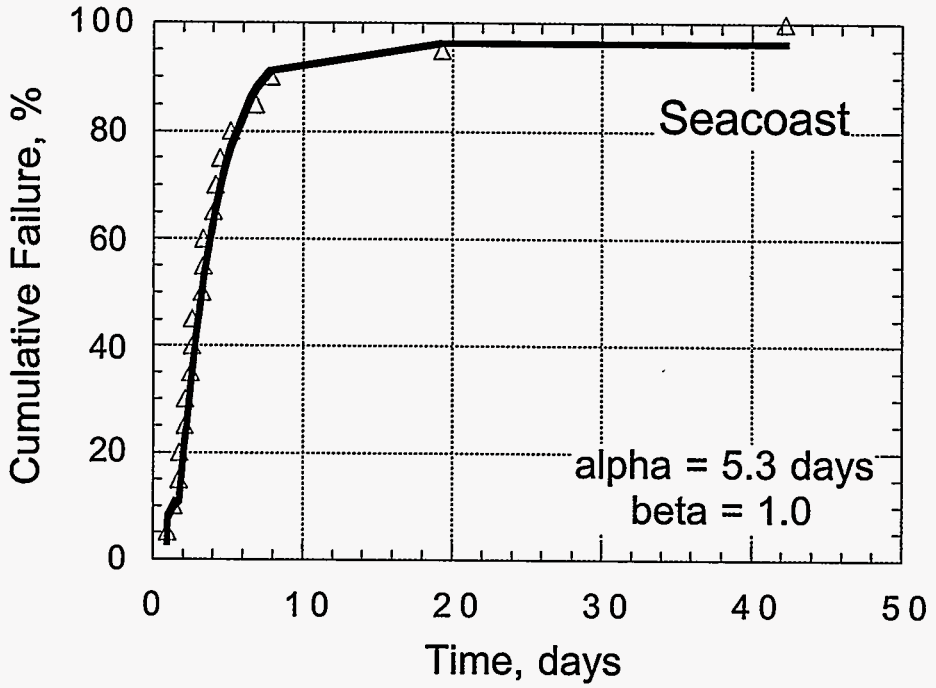

Figure 15. Cumulative wirebond failure distribution for the seacoast environment. The points are extrapolated from experimental data and the solid line represents the Weibull fit to these data.

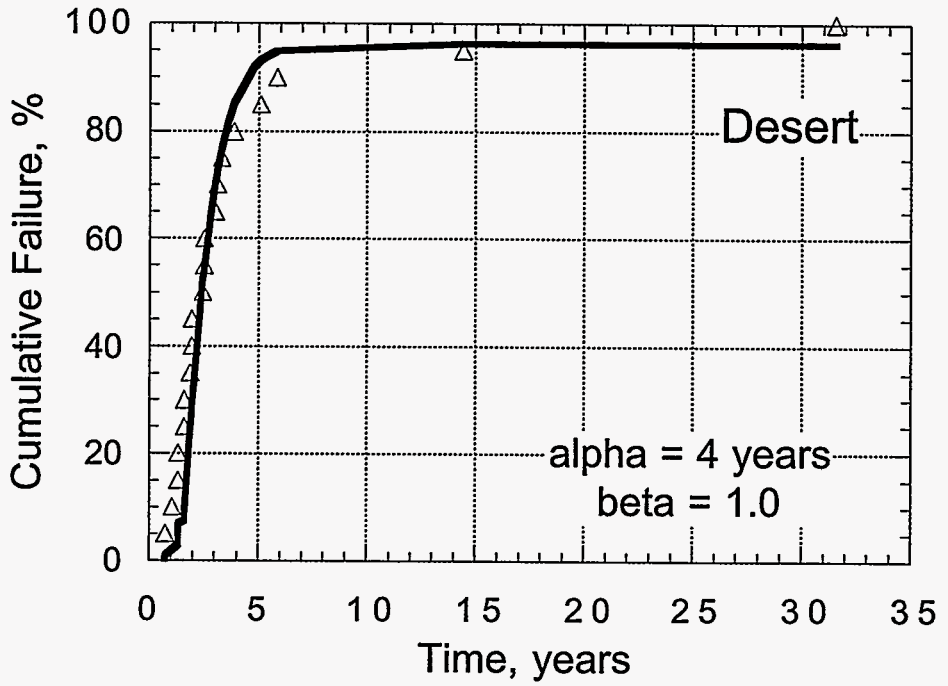

Figure 16. Cumulative wirebond failure distribution for the desert environment. The points are extrapolated from experimental data and the solid line represents the Weibull fit to these data.

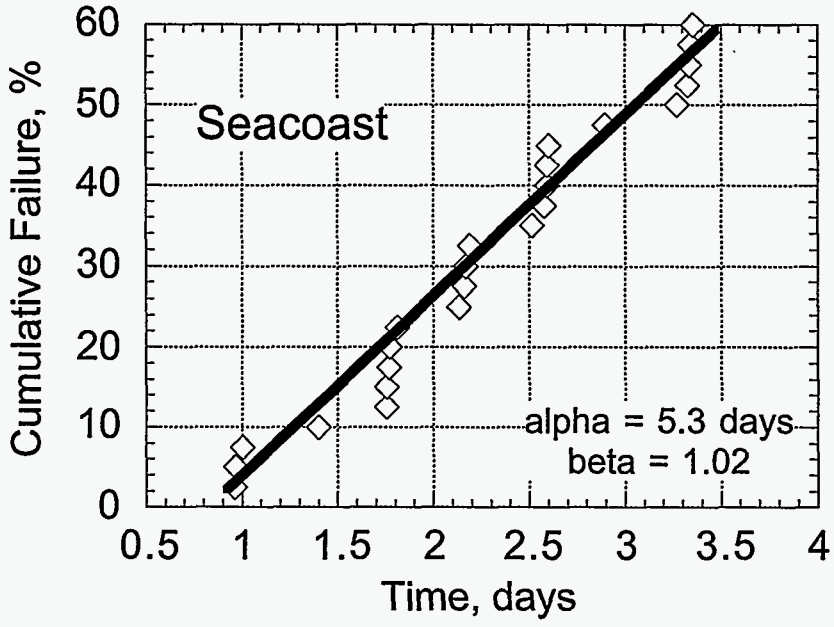

Figure 17. Expanded scale of the cumulative wirebond failure distribution for the seacoast environment (Figure 15) demonstrating the predicted linear failure rate.

Finally, to estimate the effect of corrosion on the service life of this assembly, a Monte-Carlo type simulation was performed. Such a procedure is required to characterize the probability when the first of the 10 first order or critical wirebonds will open and fail the assembly. In essence, the simulation randomly selects unopened locations and uses the appropriate Weibull distribution for the particular time step to determine if the location should then be opened. This determination is repeated as a function of time until one of the critical wirebonds opens. Then the simulation is repeated with a different random selection sequence. Statistics are recorded relative to assembly-failure time, the number of total wirebonds that have opened and when the first open occurs. The distribution of time to failure is assumed to be normal and the iterative procedure is performed until convergence of the normal statistics (mean and standard deviation) converges to a relatively constant value. For these simulations, 250 iterations was sufficient.

The Monte-Carlo results are summarized in Table 3 and shown graphically in Figure 18. Three conditions were analyzed: seacoast and desert directly using the projected experimental failure rate data (denoted as Seacoast-1 and Desert-1) and one of the desert conditions using a more typical Weibull modulus value of 3 (Desert-2). As expected for the two simulations using the projected data, with no induction time, a linear failure rate, and 5% of the population critical, the time to assembly failure is relatively short and does not approach the average wirebond failure time. This conclusion can also be understood in terms of the large statistical variance of the population - in these two cases the standard deviation is about the same as the mean which implies that a reasonable probability exists that opens will occur at very early time periods. The number of wirebond opens at assembly failure demonstrates that random nature of the corrosion simulation. That is, if uniformly distributed, the average number of opens prior to failure should be about 20. For this second desert simulation with the Weibull modulus factor of 3, the variability in time to failure is relatively much tighter and a finite induction time is predicted.

Table 3. Results from the Monte-Carlo simulation to determine assembly service life. The Seacoast and Desert-1 calculations used the projected experimental data with a more typical Weibull modulus assumed for Desert-2

Parameter	*Seacoast*	*Desert-1*	*Desert-2*
Weibull parameters	$\alpha = 5.3$ days $\beta = 1$	$\alpha = 4$ yr $\beta = 1$	$\alpha = 4$ yr $\beta = 3$
Time-to-failure			
mean	13 hr	120 da	640 da
std dev	12.5 hr	104 da	184 da
# wirebond opens			
mean	17	15	20
std dev	16	12	14
Time to first wirebond failure	1 hr	3 da	74 da

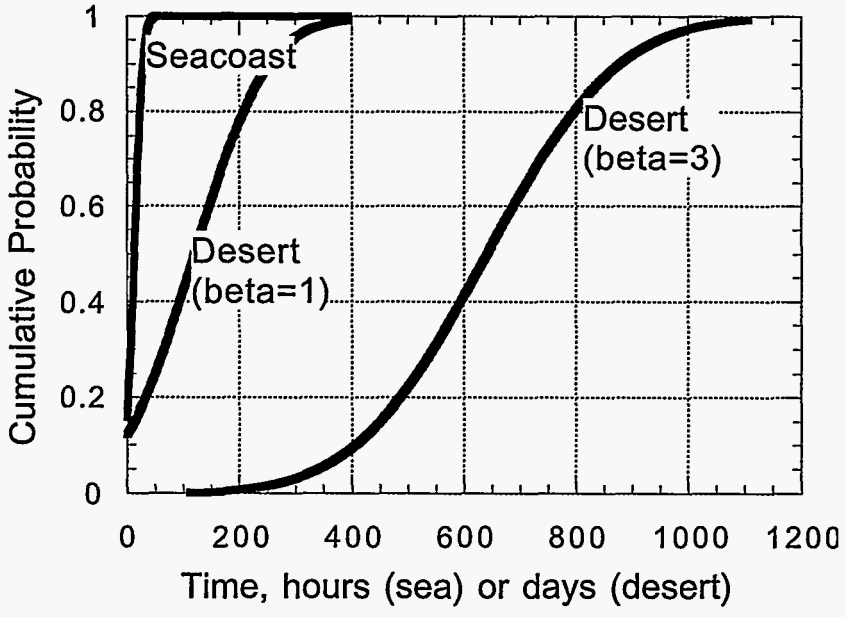

Figure 18. Calculated probability of assembly failure as a function of time for the seacoast and desert environments.

This exercise has demonstrated that stochastic corrosion-induced degradation can be successfully incorporated in classical reliability-analysis techniques: the calculated cumulative probability distributions for assembly service life are a measure of reliability. As shown in Figure 19 (short time expansion of Figure 18), for this hypothetical assembly and projected wirebond failure characteristics, the presence of non-hermetic packages would result in an unacceptable reliability -- a finite and significant probability exists (>10%) that assembly failure will occur during the initial stages of operation. If less infant mortality or latent defects existed in the wirebond population (greater shape factor), then reliability would increase.

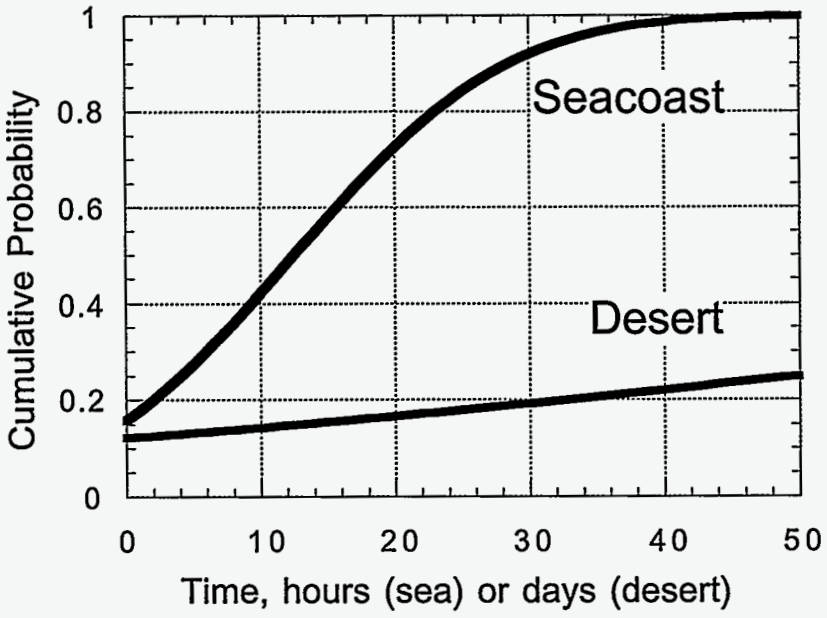

Figure 19. *Expansion of Figure 18 information showing the finite probability of assembly failure at infancy.*

SUMMARY

The effort described in this paper represents the initial part of a comprehensive project to develop effective analytical tools for predicting the effect of atmospheric corrosion on the reliability of electronic components. The specific objectives of this work were to experimentally characterize the atmospheric corrosion of aluminum-gold wirebonds and to determine if statistical-based modeling can then be used to determine reliability. At this time, the stochastic nature of Al/Au wirebond corrosion in electronic components that has been observed in the field is being characterized in the laboratory. Using accelerated aging, a preliminary assessment of the effect of three environmental factors on wirebond failure rate has been performed and an empirical rate model defined. Subsequently, a statistical treatment of the rate information was used in a Monte Carlo simulation technique to determine the service life of a hypothetical electronic assembly. This work has demonstrated that stochastic corrosion-induced degradation can be successfully incorporated in classical techniques to analyze component reliability.